Publ. Astron. Soc. Jpn (2014) 66 (1), 21 (1–12)
doi: 10.1093/pasj/pst022

Resonant excitation of tilt mode in tidally deformed disks

Shoji KATO*

2-2-2 Shikanodai-Nishi, Ikoma, Nara 630-0114

*E-mail: kato@gmail.com; kato@kusastro.kyoto-u.ac.jp

Received 2013 August 8; Accepted 2013 October 1

Abstract

In a previous paper (Kato 2013, PASJ, 65, 75), we have shown that in deformed disks a pair of trapped oscillation modes can be resonantly excited through couplings with disk deformation. In this paper we examine in what cases tilts are excited on tidally deformed disks by the above-mentioned wave–wave resonant process. The results show that tilts can be excited in various evolutional stages of tidally deformed disks, although the wave mode coupled to the tilt and the tidal wave mode contributing to the resonance change with the evolution of disk stages.

Key words: accretion, accretion disks — instabilities — negative superhumps — stars: dwarf novae — tidal deformation — tilt — waves

1 Introduction

Lubow (1991) showed that in tidally deformed disks, there is a mode–mode coupling which leads to eccentric deformation of the disk. This is the "3 : 1 resonance" and is called tidal instability. Lubow (1992) further showed that this 3 : 1 resonance can also excite tilts of disks.

In a similar context, Kato (2004, 2008) examined a wave–wave resonant coupling process in deformed disks in order to examine the origin of quasi-periodic oscillations (QPOs) observed in low-mass X-ray binaries. This wave–wave resonant excitation process in deformed disks was numerically examined by Ferreira and Ogilvie (2008) and Oktariani, Okazaki, and Kato (2010). Subsequently, Kato, Okazaki, and Oktariani (2011) and Kato (2013b) formulated the instability condition in a general way and derived the instability conditions in a simple, general form. The concept of wave energy is of importance to an understanding of the instability. The instability criterion derived is found to be formally extended to the case of magnetized disks (Kato 2014).

The wave–wave resonant process is essentially the same as Lubow's mode–mode coupling process, and is now found to be an extension of the latter to more general situations, based on a view point of wave phenomena. In fact, we can also reproduce Lubow's tidal instability, Osaki's precession of one-armed oscillations, and Lubow's excitation of tilt at the 3 : 1 resonance by the wave–wave resonant process (Kato 2013b).

A brief examination of the wave–wave resonant excitation process suggests that the process works in some realistic situation other than the 3 : 1 resonance, especially as far as excitation of tilt is concerned. This comes from the facts that in the excitation of tilts (i) a vertical p-mode oscillation is coupled to the tilt mode and (ii) the local frequency of such oscillations is not just integers of the local Keplerian frequency. From the observational point of view, on the other hand, the presence of negative superhumps has been observed in various phases of dwarf novae (e.g., Patterson et al. 1995; Ohshima et al. 2012). Negative superhumps are usually supposed to be due to the tilt of disks, although their origin is not yet understood. [See Osaki and Kato (2013a, 2013b) for extensive analyses of observational data obtained by the Kepler telescope, including those of negative superhumps.]

Considering the above situation, we examine in this paper in which situations the excitation of tilts is expected by the wave–wave resonant process on tidally deformed disks. If we restrict our attention only to applications to dwarf novae, examination of tilt excitation in the coplanar system with a circular orbit of the secondary star will be enough. By considering possible applications to such a system as Be/X-ray binaries, however, we also examine the cases where these two planes are misaligned and the orbit is eccentric. Note that what is done in this paper is only for some simplified cases. To obtain more qualitative results in realistic situations, numerical analyses evaluating growth rates by calculating coupling terms with detailed information concerning eigenfunctions of trapped oscillations are necessary. This is a subject in the near future.

To study the excitation of tilts, we must know what types of tidal wave are present on tidally deformed disks. The main factors determining the type of tidal wave are (i) the distance between the primary and secondary stars, (ii) the eccentricity of the orbit of the secondary, and (iii) the inclination between the disk plane and the orbital one. In appendix 2, the relations between the above factors and the types of tidal wave are summarized.

It is noted here that, in this paper, for the sake of simplicity, we have used the coordinate system that is centered on the primary star. If we want to apply the present results quantitatively to real observed systems, the coordinate system should be changed to the observational one.

2 Outline of wave–wave resonant processes in tidally deformed disks

Let us assume that oscillations in disks can be decomposed into normal modes. The time and angular dependences of the displacement vector, $\boldsymbol{\xi}(\boldsymbol{r}, t)$, associated with a normal mode of the oscillations are factorized as

$$\boldsymbol{\xi}(\boldsymbol{r}, t) = \Re[\hat{\boldsymbol{\xi}}(r)\exp(i\omega t)] = \Re\{\breve{\boldsymbol{\xi}}(r, z)\exp[i(\omega t - m\varphi)]\}, \quad (1)$$

where $\Re$ denotes the real part. Here, $\boldsymbol{r}$ is the cylindrical coordinates (r, φ, z), whose center is at the disk center (this is also the center of the primary star) and the z-axis is the axis of the rotating axis of the disk. We consider two oscillations specified by $\boldsymbol{\xi}^{(1)}(\boldsymbol{r}, t)$ and $\boldsymbol{\xi}^{(2)}(\boldsymbol{r}, t)$. The set of frequency, azimuthal wavenumber, and vertical node number, i.e., (ω, m, n), of each oscillation is denoted by (ω_1, m_1, n_1) and (ω_2, m_2, n_2). Generally, the radial and vertical components of a normal mode of oscillations i.e., $\xi_r(\boldsymbol{r}, t)$ and $\xi_z(\boldsymbol{r}, t)$, have different node numbers in the vertical direction. The latter component has one less number compared with the former. Here and hereafter, n is used to denote the node number of ξ_r.

Next, let us consider the component of tidal force with azimuthal wavenumber $m_{\rm D}(= \pm 1, \pm 2, \pm 3)$ and rotational frequency $\omega_{\rm D}$, where $\omega_{\rm D}/\Omega_{\rm orb} = \pm 1, \pm 2, \pm 3, \ldots, \Omega_{\rm orb}$ being the orbital frequency of the secondary star around the primary. Then, the displacement vector, $\boldsymbol{\xi}^{(\rm D)}(\boldsymbol{r}, t)$, associated with the tidal force is characterized by $(\omega_{\rm D}, m_{\rm D})$. Attention must be paid to the z-dependence of $\boldsymbol{\xi}^{(\rm D)}(\boldsymbol{r}, t)$. In coplanar systems where the disk plane and the orbital plane of the secondary coincide, the tidal potential, and thus $\xi_r^{(\rm D)}(\boldsymbol{r}, t)$, is an even function with respect to z, while in the case where these two planes are misaligned, $\xi_r^{\rm D}(\boldsymbol{r}, t)$ has both even and odd components with respect to z.

The two disk oscillations, $\boldsymbol{\xi}^{(1)}(\boldsymbol{r}, t)$ and $\boldsymbol{\xi}^{(2)}(\boldsymbol{r}, t)$, can have nonlinear resonant couplings through disk deformation, if the following resonant conditions are satisfied,[1] i.e.,

$$\omega_1 + \omega_2 + \omega_{\rm D} = 0 \quad \text{and} \quad m_1 + m_2 + m_{\rm D} = 0. \quad (2)$$

The above resonant conditions are necessary for resonant instability, but not sufficient. For the resonance leading to instability, additional conditions are necessary. Of course, the oscillations must have a common propagation region. Otherwise, the coupling is weak. More importantly, if the (E/ω)'s of the two oscillations have the same signs, i.e.,

$$\left(\frac{E_1}{\omega_1}\right)\left(\frac{E_2}{\omega_2}\right) > 0, \quad (3)$$

the resonant coupling leads to instability (Kato 2013b). Here, E is the wave energy defined, e.g., for the wave of $\boldsymbol{\xi}^{(1)}(\boldsymbol{r}, t)$ by,

$$E_1 = \int \frac{1}{2}\omega_1 \left[\omega_1 \rho_0 \hat{\boldsymbol{\xi}}^{(1)*}\hat{\boldsymbol{\xi}}^{(1)} - i\rho_0 \hat{\boldsymbol{\xi}}^{(1)*}(\boldsymbol{u}_0 \cdot \nabla)\hat{\boldsymbol{\xi}}^{(1)}\right] dV$$
$$\sim \int \frac{1}{2}\omega_1 \left[(\omega_1 - m_1\Omega)\left(\hat{\boldsymbol{\xi}}_r^{(1)*}\hat{\boldsymbol{\xi}}_r^{(1)} + \hat{\boldsymbol{\xi}}_z^{(1)*}\hat{\boldsymbol{\xi}}_z^{(1)}\right)\right] dV, \quad (4)$$

where $\boldsymbol{u}_0(\boldsymbol{r})$ is the velocity on the unperturbed disk, i.e., $\boldsymbol{u}_0(\boldsymbol{r}) = [0, r\Omega(r), 0]$, and the asterisk denotes the complex conjugate; the integration should be performed over the whole volume where the (trapped) oscillations exist. The condition, $(E_1/\omega_1)(E_2/\omega_2) > 0$, is roughly equal to $(\omega_1 - m_1\Omega)(\omega_2 - m_2\Omega) > 0$ [see equation (4)].

To evaluate the growth rate, we must calculate the magnitude of the coupling. The efficiency of coupling among

[1] In Kato, Okazaki, and Oktariani (2011) and Kato (2013a) we have adopted as the resonant conditions, $\omega_2 = \omega_1 \pm \omega_{\rm D}$ and $m_2 = m_1 \pm m_{\rm D}$. However, since the signs of ω and m can be taken to be negative, the forms of expression (2) are convenient for general arguments, and in Kato (2013b) we have adopted expression (2). Here and hereafter, we adopt expression (2).

three modes of oscillations, $\boldsymbol{\xi}^{(1)}$, $\boldsymbol{\xi}^{(2)}$, and $\boldsymbol{\xi}^{(\mathrm{D})}$, is measured by W, defined by (Kato 2013b)

$$W = \int \hat{\boldsymbol{\xi}}^{(1)} \cdot \boldsymbol{C}(\hat{\boldsymbol{\xi}}^{(2)}, \hat{\boldsymbol{\xi}}^{(\mathrm{D})}) dV = \int \hat{\boldsymbol{\xi}}^{(2)} \cdot \boldsymbol{C}(\hat{\boldsymbol{\xi}}^{(1)}, \hat{\boldsymbol{\xi}}^{(\mathrm{D})}) dV, \quad (5)$$

where $\boldsymbol{C}(\hat{\boldsymbol{\xi}}^{(2)}, \hat{\boldsymbol{\xi}}^{(\mathrm{D})})$, for example, is the nonlinear terms of the wave equation of $\hat{\boldsymbol{\xi}}^{(1)}$, representing the effects of coupling between $\hat{\boldsymbol{\xi}}^{(2)}$ and $\hat{\boldsymbol{\xi}}^{(\mathrm{D})}$ on $\hat{\boldsymbol{\xi}}^{(1)}$. The volume integration of the product of $\hat{\boldsymbol{\xi}}^{(1)}$ and $\boldsymbol{C}(\hat{\boldsymbol{\xi}}^{(2)}, \hat{\boldsymbol{\xi}}^{(\mathrm{D})})$ is related to growth of the oscillation of $\boldsymbol{\xi}^{(1)}$ (Kato 2013b).

An explicit expression for W is (Kato 2004, 2008, 2013b)

$$W = W^{\psi} + W^{\mathrm{P}} + W^{\mathrm{T}}, \quad (6)$$

where W^{ψ}, W^{P}, and W^{T} are expressed, respectively, in the case of isothermal oscillations, as

$$W^{\psi} = -\int \rho_0 \xi_i^{(1)} \xi_j^{(2)} \xi_k^{\mathrm{D}} \frac{\partial^3 \psi_0}{\partial r_i \partial r_j \partial r_k} dV, \quad (7)$$

$$W^{\mathrm{P}} = \int p_0 \frac{\partial \xi_i^{(1)}}{\partial r_k} \left[\frac{\partial \xi_k^{(2)}}{\partial r_j} \frac{\partial \xi_j^{(\mathrm{D})}}{\partial r_i} + \frac{\partial \xi_j^{(2)}}{\partial r_i} \frac{\partial \xi_k^{(\mathrm{D})}}{\partial r_j} \right] dV, \quad (8)$$

$$W^{\mathrm{T}} = -\int \rho_0 \xi_i^{(1)} \xi_j^{(2)} \frac{\partial^2 \psi_{\mathrm{D}}}{\partial r_i \partial r_j} dV, \quad (9)$$

where $\rho_0(\boldsymbol{r})$, $p_0(\boldsymbol{r})$, and $\psi_0(\boldsymbol{r})$ are, respectively, the density, pressure, and gravitational potential in the unperturbed disk, and ψ_{D} is the part of the gravitational potential perturbation caused by the tidal force. It is important to note that the roles of $\hat{\boldsymbol{\xi}}^{(1)}$ and $\hat{\boldsymbol{\xi}}^{(2)}$ in W are commutative, as shown in equation (5), which can be shown directly from equations (7)–(9). This commutability is the reason why the instability criterion is written in a simple form such as $(E_1/\omega_1)(E_2/\omega_2) > 0$. The coupling term, W, has no influence on the stability criterion; it affects only growth rate. The growth rate of the ω_1 and ω_2 oscillations is given by (Kato 2013b)

$$\left(\frac{\omega_1 \omega_2}{16 E_1 E_2} \right)^{1/2} |\Im(W)|, \quad (10)$$

where $\Im(W)$ denotes the imaginary part of W. It is noted that the growth rate is proportional to the amplitude (a complex quantity in general) of the tidal deformation.

Finally, it is noted that in the case of coplanar systems, the difference between n_1 and n_2 needs to be zero or even for resonantly interacting oscillations. This is because if the difference is odd, the product of $\boldsymbol{\xi}^{(1)}$ and $\boldsymbol{\xi}^{(2)}$ in W is an odd function with respect to z, and W vanishes since $\boldsymbol{\xi}^{(\mathrm{D})}$ is an even function in coplanar systems. This can be shown by detailed examinations of the expression for W. In the case of misaligned systems, however, $\boldsymbol{\xi}^{(\mathrm{D})}$ has both even and odd components with respect to z, and thus W does not vanish generally even if the difference between n_1 and n_2 is odd.

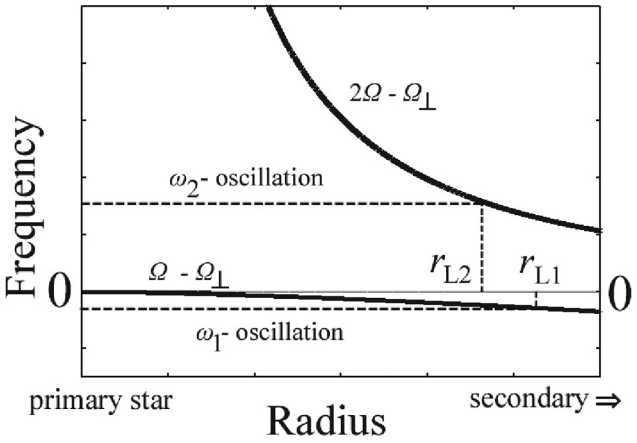

Fig. 1. Schematic diagram showing the propagation regions of ω_1 oscillation (tilt mode) and ω_2 oscillation. The scales of coordinates are arbitrary, and are not linear. The set (m_1, n_1) of the ω_1 oscillation is (1, 1) and that adopted for ω_2 oscillation is (2, 1). The outer edges of the propagation regions of the ω_1 and ω_2 oscillations are denoted by r_{L1} and r_{L2}, respectively.

3 Tilt mode trapped

Here and hereafter, the ω_1 oscillation is taken to be the tilt mode [in other terminology, it is the mode of the corrugation wave (e.g., Kato 2001; Kato et al. 2008)]. That is, we adopt $m_1 = 1$ and $n_1 = 1$. The local dispersion relation[2] shows that this mode has a propagation region in the radial region specified by $\omega_1 - \Omega < -\Omega_\perp$, where $\Omega_\perp(r)$ is the vertical epicyclic frequency and larger than the angular velocity of disk rotation, $\Omega(r)$, in tidally deformed disks. Since $\Omega - \Omega_\perp < 0$ and tends to zero in the innermost region of the disks, the tilt mode with a given frequency $\omega_1 (< 0)$ is trapped inside a radius, say r_{L1}, where ω_1 becomes equal to $\Omega - \Omega_\perp$, i.e., $\omega_1 = (\Omega - \Omega_\perp)_{\mathrm{L1}}$, the subscript L1 denoting the value at r_{L1}. This is schematically shown in figure 1.[3] It should be noted that this ω_1 oscillation has

[2] The local dispersion relation for isothermal perturbations in vertically isothermal disks is (e.g., Okazaki et al. 1987; Kato 2001; Kato et al. 2008)

$$[(\omega - m\Omega)^2 - \kappa^2][(\omega - m\Omega)^2 - n\Omega_\perp^2] = c_{\mathrm{s}}^2 k^2 (\omega - m\Omega)^2,$$

where κ and $\Omega_\perp$ are, respectively, the horizontal and vertical epicyclic frequencies, and k is the radial wavenumber of the oscillations. This local dispersion relation shows the presence of oscillation modes propagating in the region of $(\omega - m\Omega)^2 > n\Omega_\perp^2 (n = 1, 2, 3 \ldots)$, since $\Omega_\perp$ is always larger than κ.

[3] If ω_1 is smaller than the value of $\Omega - \Omega_\perp$ at the disk outer edge, the propagation region is terminated at the disk edge.

a negative value of E_1/ω_1, i.e., $E_1/\omega_1 < 0$, since $\omega - \Omega < 0$ [see equation (4)].

Here, we derive a rough relation between ω_1 (or r_{L1}) and temperature (or acoustic speed c_s) in the disks by the WKB method (for details of the WKB method, see Morse & Feshbach 1953). The outline of the method is given in appendix 1. The results show that the trapping condition (capture condition) is given by

$$\int_{r_i}^{r_{L1}} Q^{1/2} dr = \pi \left(n_r + \frac{3}{4} \right) \qquad (n_r = 0, 1, 2, \ldots), \tag{11}$$

where

$$Q = \frac{[(\omega - m\Omega)^2 - \kappa^2][(\omega - m\Omega)^2 - n\Omega_\perp^2]}{c_s^2(\omega - m\Omega)^2}. \tag{12}$$

Hereafter we restrict our attention to the fundamental oscillation mode ($n_r = 0$) in the radial direction. The outer edge of the propagation region, r_{L1}, is the turning point of Q, where $Q(r)$ changes its value from positive to negative. In the trapping condition (11) the radial velocity associated with the oscillation, u_r, has been taken to vanish at the inner edge.[4] In the present problem, $m = 1$ and $n = 1$, since we are interested in the tilt mode, and we adopt[5]

$$\Omega - \kappa = \frac{3}{4} q \Omega \left(\frac{r}{a} \right)^3, \quad \Omega - \Omega_\perp = -\frac{3}{4} q \Omega \left(\frac{r}{a} \right)^3, \tag{13}$$

where q is the mass ratio of the secondary to the primary, and a is the mean separation between the primary and secondary stars. It is noted that since the outer edge of the trapping region, r_{L1}, is the turning point of $Q(r)$, r_{L1} and ω_1 are related by $Q(r_{L1}) = 0$. In the present problem, the relation is

$$\omega_1 = (\Omega - \Omega_\perp)_{L1}. \tag{14}$$

This relation between trapping radius (capture radius), r_{L1}, and eigenfrequency, ω_1, is shown in figure 2 for three cases of $q = 0.1$, 0.2, and 0.3.

For the sake of simplicity, the acoustic speed c_s in disks is taken to be constant, and the inner edge r_i is taken to be zero. Then, the trapping condition [equation (11)] is a relation between r_{L1}/a and $c_s/(GM/a)^{1/2}$ with a parameter q, where G is the gravitational constant and M is the mass of the primary star. The relation is shown in figure 3 for three cases of $q = 0.1$, 0.2, and 0.3.

[4] If the radial gradient of the radial velocity associated with the oscillation is taken to vanish at the inner edge, i.e., $du_r/dr = 0$, the right-hand side of equation (11) is $\pi(n_r + 1/4)$ instead of $\pi(n_r + 3/4)$.

[5] Equations (13) are crude approximations, based on an expansion of the tidal potential in r/a, as pointed out by the referee. More accurate expressions are necessary for more detailed calculations.

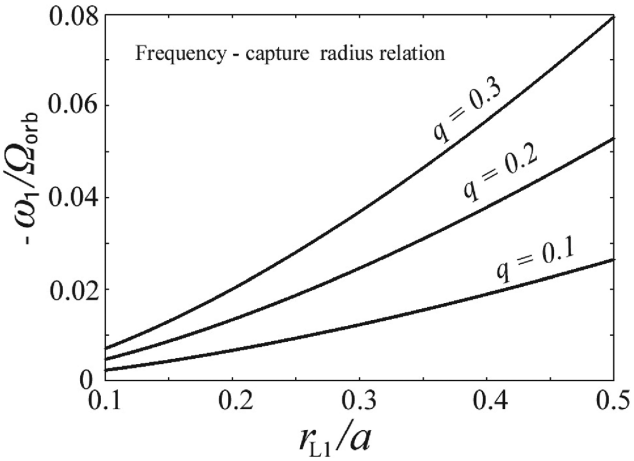

Fig. 2. The relation between the frequency, ω_1/Ω_{orb}, and the capture (trapping) radius, r_{L1}, of the tilt mode. Three cases of the mass ratio of the secondary to the primary, i.e., $q = 0.1$, 0.2, and 0.3 are shown.

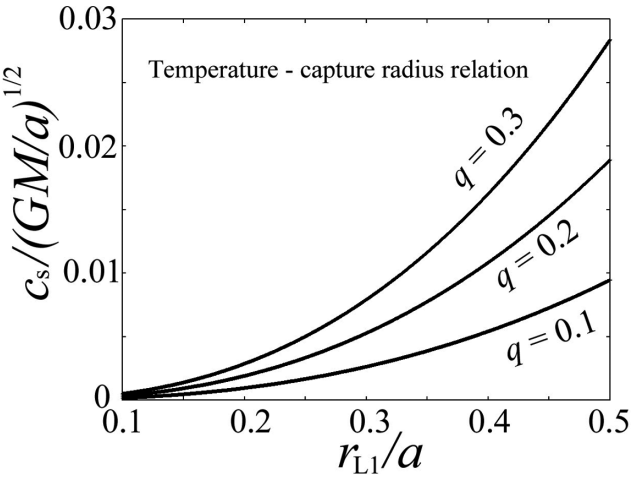

Fig. 3. Capture radius (trapping radius) r_{L1}–acoustic speed c_s relation obtained by the WKB method for the tilt mode with $n_r = 0$. Three cases of $q = 0.1$, 0.2, and 0.3 are shown.

4 Counterpart of tilt mode, i.e., ω_2 oscillation

In order for the ω_1 oscillation (tilt) mentioned above to be excited by the wave–wave resonant process, the ω_2 oscillation must also have a negative value of E_2/ω_2 so that the excitation condition $(E_1/\omega_1)(E_2/\omega_2) > 0$ is satisfied. Here and hereafter, we consider vertical p-mode oscillations propagating in their inner propagation region, since these oscillations have $E_2/\omega_2 < 0$ there. In the case of isothermal oscillations in vertically isothermal disks, their propagation region is specified by $\omega_2 < m_2\Omega - \sqrt{n_2}\Omega_\perp$ (see the local dispersion relation given in footnote 2).

Hereafter, we concentrate our attention on the ω_2 oscillations with $n_2 = 1$, $n_2 = 2$, or $n_2 = 3$. If $m_2 \geq 2$, ω_2 is positive, and the propagation region of these oscillations is between the inner edge of the disk and the radius where $\omega_2 = m_2\Omega - \sqrt{n_2}\Omega_\perp$. The latter radius is denoted by

r_{L2}, i.e., $\omega_2 = (m_2\Omega - \sqrt{n_2}\Omega_\perp)_{L2}$. The propagation region of the ω_2 oscillation with $m_2 = 2$ and $n_2 = 1$ is schematically shown in figure 1.

Unlike the case of ω_1 oscillations, we do not discuss here the trapping condition of ω_2 oscillations for the following reasons. The frequency of the ω_2 oscillation which will be considered here is much higher than that of the ω_1 oscillation, and is comparable with the frequency of disk rotation. Related to this, the trapped oscillations will have higher overtones in the radial direction, i.e., they will have many nodes in the radial direction. In other words, for any frequency ω_2 required from the resonant condition, there will always be a trapped oscillation with frequency close to ω_2. Hence, we assume here that the ω_2 oscillation required from the resonant condition roughly satisfies the trapping conditions.

5 Resonant conditions and trapping (capture) radius

Next, let us consider the resonant conditions. The frequency ω_1 and the outer trapping radius (capture radius) of the ω_1 oscillation, r_{L1}, are related with $\omega_1 = (\Omega - \Omega_\perp)_{L1}$, and ω_2 and r_{L2} are related with $\omega_2 = (m_2\Omega - \sqrt{n_2}\Omega_\perp)_{L2}$, as mentioned before. Furthermore, we consider the tidal wave whose frequency ω_D is $n\Omega_{orb}$ ($n = \pm1, \pm2, \pm3, \ldots$) and whose azimuthal wavenumber is m_D. Then, the resonant condition, $\omega_1 + \omega_2 + \omega_D = 0$, is written as

$$(\Omega - \Omega_\perp)_{L1} + (m_2\Omega - \sqrt{n_2}\Omega_\perp)_{L2} + n\Omega_{orb} = 0, \tag{15}$$

and $m_1 + m_2 + m_D = 0$ gives

$$m_D = -(1 + m_2). \tag{16}$$

The next problem is to identify in which case of the r_{L1} and r_{L2} relation the growth rate of resonant oscillations becomes maximum. The growth rate is given by equation (10) and can be calculated by using the coupling constant W, with eigenfunctions of the ω_1 and ω_2 oscillations and the form of the tidal wave. This will be done in the near future. The following considerations concerning the limiting case of zero-temperature disks, however, suggest that the growth rate will be high when r_{L1} and r_{L2} are close in radius, i.e., $r_{L1} \sim r_{L2}$.

Let us first consider the nonlinear coupling between the ω_1 oscillation (with $m_1 = 1$ and $n_1 = 1$) and the tidal wave with ω_D (with an arbitrary m_D and $n_D = 0$). The coupling gives rise to a vertical p-mode oscillation of frequency $\omega_1 + \omega_D$ with azimuthal wavenumber $m_1 + m_D$, the vertical node number being unity. In the limit of zero-temperature disks, the disks respond resonantly to this vertical forced oscillation at the radii where $[(\omega_1 + \omega_D) - (m_1 + m_D)\Omega]^2 - \Omega_\perp^2 = 0$ is satisfied (e.g., Kato 2008). If we introduce ω_2 and m_2 defined by the resonant conditions, $\omega_1 + \omega_2 + \omega_D = 0$ and $m_1 + m_2 + m_D = 0$, the radii of the above resonant response are specified by $(\omega_2 - m_2\Omega)^2 - \Omega_\perp^2 = 0$. One of the two radii which satisfy this condition is r_{L2}. Similarly, let us consider the coupling between the ω_2 oscillation and the tidal wave. This gives rise to the ω_1 oscillation with $m_1 = 1$ and $n_1 = 1$. To this forced oscillation with frequency ω_1, the disk sharply responds at the radii defined by $(\omega_1 - \Omega)^2 - \Omega_\perp^2 = 0$ ($m_1 = 1$ and $n_1 = 1$). One of these radii is r_{L1}. These considerations show that in the limiting case of zero-temperature disks, the resonant coupling between ω_1 and ω_2 oscillations through disk deformation occurs if $r_{L1} = r_{L2}$ can be realized (Lubow 1991, 1992). In disks with a finite temperature, however, the resonance is not sharply restricted only to the case of $r_{L1} = r_{L2}$, since the resonant region is widened by temperature effects (e.g., Meyer-Vernet & Sicardy 1987). The growth rate, however, will be high in the case where $r_{L1} \sim r_{L2}$.

Taking $r_{L1} \sim r_{L2}$ and representing both radii by a symbol r_L, we have from equation (15)

$$\frac{\Omega_L}{\Omega_{orb}} \sim -\frac{n}{m_2 - \sqrt{n_2}}, \tag{17}$$

if the difference between Ω and $\Omega_\perp$ is neglected, where Ω_L is the value of Ω at $r = r_L$. It is noted that n needs to be a negative integer in the present case, since we are here interested in cases where $m_2 - \sqrt{n_2}$ is positive. In the case of dwarf novae, the disk is known to be roughly truncated by the tidal instability of the "3 : 1 resonance" at the radius where $\Omega/\Omega_{orb} \sim 3:1$ (Lubow 1991). Hence, hereafter, we restrict our attention only to resonances which occur inside the radius of $\Omega_L/\Omega_{orb} = 3$, i.e., to the cases where $\Omega_L/\Omega_{orb} > 3.0$. Furthermore, resonances which occur only in misaligned systems are considered separately from those that occur in both coplanar and misaligned systems.

5.1 Coplanar cases

Two cases of $(m_2, n_2) = (2, 1)$ and $(2, 3)$ are considered. In the former case we have $\Omega_L/\Omega_{orb} \sim -n$ [see equation (17)], which is equal to or larger than 3 for $n \leq -3$. For three cases of $n = -3, -4$, and -5, some characteristic quantities related to the resonant radius (r_L/a) and the mode of tidal wave required (m_D and ω_D) are shown in the upper part (the second to fourth lines) of table 1. For the resonance shown in the second line ($n = -3$), the tidal waves required are those with $\omega_D = -3\Omega_{orb}$ and $m_D = -3$. These tidal waves are practically equivalent to those with $\omega_D = 3\Omega_{orb}$

Table 1. Normalized capture radius (trapped radius), r_L/a, of tilts for various set of (m_2, n_2) and n.

Inclination	(m_2, n_2)	$n(\equiv \omega_D/\Omega_{orb})$	m_D	Ω_L/Ω_{orb}	r_L/a	R/D	Eccentricity
$\delta = 0$	(2, 1)	-3	-3	3	0.48	P_3	e^0
		-4	-3	4	0.40	P_3	e^1
		-5	-3	5	0.34	P_3	e^2
	(2, 3)	-1	-3	3.73	0.42	P_3	e^2
		-2	-3	7.46	0.26	P_3	e^1
		-3	-3	11.19	0.20	P_3	e^0
$\delta \neq 0$	(2, 2)	-2	-3	3.41	0.44	P_4	e^0
		-3	-3	5.12	0.34	P_4	e^1
		-4	-3	6.83	0.28	P_4	e^0

and $m_D = 3$, since there is no change of waves by changing the signs of ω_D and m_D simultaneously.

If the orbit of the secondary star around the primary is circular, the tidal waves which remain in the limit of the secondary being far away from the primary are two-armed ($m_D = 2$) with $\omega_D = 2\Omega_{orb}$ [see the terms of P_2 in the limit of coplanar systems ($\delta = 0$) in equation (A14) in appendix 2]. If the secondary is closer to the primary, three-armed ($m_D = 3$) tidal waves with $\omega_D = 3\Omega_{orb}$ appear [see the terms of P_3 of equation (A15) in appendix 2]. The tidal wave required in the case of the second line in table 1 corresponds to this case, and thus symbols P_3 and e^0 (no eccentricity) are indicated in the last two columns on the second line of table 1. It is noted that the tilt by this resonance is nothing but what was considered by Lubow (1992) and briefly mentioned by Kato (2013b).

The resonance of the third line, i.e., $n = -4$ and $m_D = -3$, shows that the ω_D required for the resonance is $\omega_D = -4\Omega_{orb}$ [see equation (17)], and the m_D required is -3. That is, the $|\omega_D/\Omega_{orb}|$ required is larger than $|m_D|$. Deviation of ω_D from $\omega_D/\Omega_{orb} = m_D$ cannot be realized as long as $e = 0$, i.e., eccentric orbits of the secondary are necessary. In the case of eccentric orbits, the deviation of the tidal force from a form proportional to $\exp[i(m_D\Omega_{orb}t - m_D\varphi)]$ is realized by two effects. One is that the motion of the secondary on the orbit is not at a constant pace [see equation (A20) in appendix 2]. The second is that the distance between the primary and the secondary, D, changes with time [see equation (A22) in appendix 2]. If these are taken into account till the terms of e^1, the tidal force ψ_D, which is given by equation (A8) in appendix 2, has terms proportional to $\exp[i(m_D \pm 1)\Omega_{orb}t - im_D\varphi]$. That is, the tidal waves with $\omega_D = (m_D \pm 1)\Omega_{orb}$ appear in addition to those with $\omega_D = m_D\Omega_{orb}$. The case shown in the third line of table 1 requires such effects of eccentricity e, and thus e^1 is indicated in the last column of table 1.

If the expansion with respect to e is taken into account till the terms of e^2, tidal waves with $\omega_D = (m_D \pm 2)\Omega_{orb}$ appear in addition to those with $\omega_D = m_D\Omega_{orb}$ and $\omega_D = (m_D \pm 1)\Omega_{orb}$. The fourth line in table 1 is a case where such tidal waves are required, and e^2 is indicated in the last column of table 1.

In the case of $(m_2, n_2) = (2, 3)$, we have $\Omega_L/\Omega_{orb} \sim -n/(2-\sqrt{3})$ [see equation (17)], and the ratio Ω_L/Ω_{orb} becomes larger than 3.0 for $n \leq -1$. Some characteristic quantities related to the resonant radius and the mode of tidal wave required are shown in the middle part (the fifth to seventh lines) of table 1.

The radial positions of resonant excitation of the tilt mode by the various processes mentioned above are plotted on the r_L–c_s diagram in figure 4. It is noted that the plots are on the r_L–c_s curve given in figure 3.

5.2 Misaligned cases

If the disk and orbital planes are misaligned (i.e., $\delta \neq 0$), the tilt mode ($m_1 = 1$ and $n_1 = 1$) can be resonantly excited even when the ω_2 oscillation to be paired with the tilt is plane-symmetric (i.e., $n_2 =$ even), since the tidal force has a plane-asymmetric term [see that P_2, P_3, ... given in appendix 2 have terms proportional to $\sin\gamma$, which are those of odd powers of z]. Here, we consider, in particular, the case of $(m_2, n_2) = (2, 2)$. In this case we have $\Omega_L/\Omega_{orb} = -n/(2-\sqrt{2})$ [see equation (17)]. Three cases of $n = -2$, -3, and -4 are considered and some characteristic quantities related to the resonant radius and the mode of tidal wave required are shown in the lower part (the eighth to tenth lines) of table 1.[6]

Let us first consider the case where the orbit of the secondary is circular ($e = 0$). As shown in appendix 2, the tidal force resulting from $\delta \neq 0$ (but $\delta \ll 1$ is assumed) has a term proportional to $\exp[i(2\Omega_{orb}t - \varphi)]$ in P_2 [see equation (A14)], terms proportional to $\exp[i(3\Omega_{orb}t - 2\varphi)]$

[6] It is noted that the resonant excitation discussed in the coplanar cases is still present in misaligned systems. The resonant processes to be mentioned below are in addition to this.

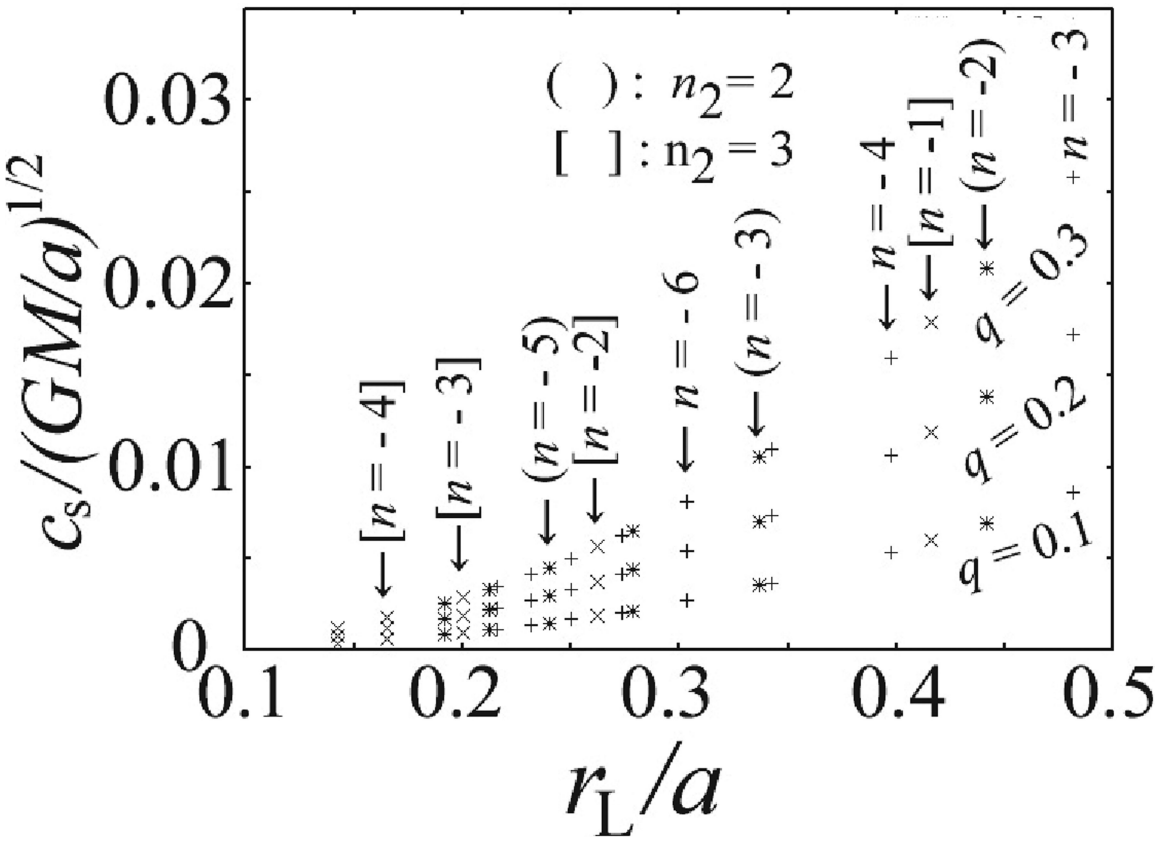

Fig. 4. Positions of various resonances in the radius–temperature diagram. Two capture radii of the set of two oscillations, r_{L1} and r_{L2}, are taken to be the same and denoted by r_L. The azimuthal wavenumber of the ω_2 oscillation is taken to be $m_2 = 2$ in all cases, and for n_2 of the ω_2 oscillation three cases are considered. The resonant positions in the cases of $n_2 = 1$ are shown by "+," those in the cases of $n_2 = 2$ by "×," and those in the cases of $n_2 = 3$ by "∗". The value of $n(\equiv \omega_D/\Omega_{orb})$ required is indicated for each resonance by attaching symbols after the arrow. The three sequences of plots show the difference of the mass ratio of the two stars, i.e., $q = 0.3$, 0.2, and 0.1 from the upper sequence to the lower one. It is noticed that the resonant points are along the r_L–c_s curves given in figure 3.

and $\exp[i(\Omega_{orb}t - 2\varphi)]$ in P_3 [see equation (A15)], and terms proportional to $\exp[i(4\Omega_{orb}t - 3\varphi)]$ and $\exp[i(2\Omega_{orb}t - 3\varphi)]$ in P_4, although a detailed expression for P_4 is not presented in appendix 2.

The tidal force required in the case of the eighth line of table 1 is proprotional to $\exp[i(2\Omega_{orb}t - 3\varphi)]$ (i.e., $n = -2$ and $m_D = -3$). As mentioned in the above paragraph, the tidal force resulting from $\delta \neq 0$ has such a term in P_4 with $e = 0$. That is, the tidal force required in the case of the eighth line of table 1 appears in P_4 with $e = 0$. Thus, P_4 and e^0 are indicated in the last two columns of the eighth line of table 1. In the case of the ninth line of table 1, however, eccentricity is necessary, since the n and m_D required in this case are the same (i.e., $n = -3$ and $m_D = -3$, in other words, $n = 3$ and $m_D = 3$), and such a tidal force does not appear from the term resulting from $\delta \neq 0$ if $e = 0$. Such a tidal force, however, appears in P_4 if the effects of eccentricity are taken into account till the terms proportional to e^1. To emphasize this point, P_4 and e^1 are noted in the last two columns of the ninth line of table 1. The tidal force required in the case of the tenth line is proportional to $\exp[i(4\Omega_{orb}t - 3\varphi)]$. Such force is present in P_4 even when $e = 0$, as mentioned in the above paragraph. Thus, P_4 and e^0 are noted in the last two columns of the tenth line of table 1.

The radial positions of resonant excitation of tilt in the cases mentioned above are also plotted on the r_L–c_s diagram in figure 4.

Although tilts which are excited at various capture radius, r_L, are listed in table 1 and figure 4, this does not mean that all of them are excited to an observable level in dwarf novae. In close binary systems such as dwarf novae, the eccentricity of the orbit of the secondary star is small, i.e., $e \sim 0$. Hence, in the cases labeled e^1 or e^2 in the last column of table 1, the amplitude of the tidal deformation is small and thus the growth rate of the tilt will be small. In addition, in the case of dwarf novae, the inclination of the orbital plane to the disk plane is small, i.e., $\delta \sim 0$. Hence, the tilts shown in the last three lines of table 1 are also not expected with observable amplitudes. In summary, the tilts

which will be important in dwarf novae will be those of the second line ($\Omega_L/\Omega_{orb} = 3$ and $r_L/a = 0.48$) and the seventh line ($\Omega_L/\Omega_{orb} = 11.19$ and $r_L/a = 0.20$), and also those of the third line ($\Omega_L/\Omega_{orb} = 4$ and $r_L/a = 0.40$) and the sixth line ($\Omega_L/\Omega_{orb} = 7.46$ and $r_L/a = 0.26$). The excitation of tilt at $\Omega_L/\Omega_{orb} = 3$ is nothing but what was pointed out by Lubow (1992). A numerical evaluation of growth rate [given by equation (10)] in the above four cases will be made in the future.

In Be/X-ray systems, the Be-star disk and the orbital plane of a compact star (in general a neutron star) is generally misaligned, and, further, a secondary star has a large eccentric orbit. In colliding or merging black hole binaries, each black hole will have its own disk, although the system as a whole will be surrounded by a common envelope. In Be/X-ray stars, for example, in addition to normal outbursts, giant outbursts which occur less frequently are observed. The giant outbursts are supposed to be due to an interaction between a warped precessing Be-star disk and a secondary star which has a large eccentric orbit (Moritani et al. 2013). Considering such situations, it will be important to examine the wave–wave resonant process in disks whose plane is inclined from the orbital plane of an eccentric binary system. In such systems, resonant excitations of tilt at the various radii listed in table 1 will have comparable growth rates.

6 Discussions

We have demonstrated that on tidally deformed disks, slowly retrograding tilts are generated by wave–wave resonant processes at various phases of disk temperature (see figure 4). Our analyses in this paper, however, are only for special cases of $r_{L1} = r_{L2}$. That is, we have assumed that for a trapped tilt mode whose capture radius is r_{L1}, there is always trapped ω_2 oscillation whose capture radius r_{L2} is sufficiently close to r_{L1}. In real situations, there may be no such ω_2 oscillations, depending mainly on the temperature distribution on disks. Even in such cases, unless the difference between r_{L1} and r_{L2} is too large, resonant instability occurs, although the growth rate will decrease with increasing separation between r_{L1} and r_{L2}. This comes from the following situations. We can calculate the coupling factor, W [see equation (5)], of the resonant interaction and thus the growth rate given by equation (10), if we know the eigenfunctions of ω_1 and ω_2 oscillations and the functional form of tidal waves, even if $r_{L1} \neq r_{L2}$. Based on conjecture in the case of zero-temperature disks, however, we suppose that the growth rate is high in the case of $r_{L1} \sim r_{L2}$. Conversely, there will be cases where $r_{L1} = r_{L2}$ is realized for ω_1 and ω_2 which deviate slightly from the resonant condition, $\omega_1 + \omega_2 + \omega_D = 0$. Even in such cases, resonant instability occurs, since in finite-temperature disks the resonant instability is not sharply restricted only to the case of $\omega_1 + \omega_2 + \omega_D = 0$, i.e., the resonance is broadened in frequency space. Considering the above situations, we think that in real disks the resonant instability occurs in the finite region around each discrete point in figure 4.

Next, it is noted why, in the case of excitation of the tilt mode, we have great variety in the resonant radius and thus in the precession frequency of the tilt, compared with the case of the excitation of one-armed p-mode oscillation.[7] Let us consider, for simplicity, the case of coplanar systems ($\delta = 0$). The oscillations describing the tilt are asymmetric with respect to the equatorial plane. Hence, the ω_2 oscillation must also be asymmetric ($n_1 = 1$) with respect to the equatorial plane, since the tidal force is plane-symmetric ($\delta = 0$) with respect to the equatorial plane in coplanar cases. This means that n_2 of the ω_2 oscillation must be odd (not $n_2 = 0$). Hence, if we consider a vertical p-mode oscillation as the ω_2 oscillation, the mode has a frequency given by $\omega_2 = (m_2\Omega - \sqrt{n_2}\Omega_\perp)_{L2}$, n_2 being 1, 3, ... This frequency is not an integer times Ω_{L2}, and can have various values as a result of the variety of m_2 and n_2.

Unlike the above case of tilt excitation, in the case of excitation of one-armed p-mode oscillation, the ω_2 oscillation contributing to the excitation needs to be plane-symmetric, in the case of coplanar systems. Hence, typical modes of the ω_2 oscillation are those with $n_2 = 0$. This makes the variety of ω_2 oscillations which can contribute to resonance less than that in the case of excitation of tilts.

Observations of dwarf novae show that they have various types of time variations. One well-studied time variation is (positive) superhumps, which appear in the superoutburst phase. The origin of the time variations is the excitation of low-frequency one-armed progressive p-mode oscillations (Osaki 1985) associated with the "3 : 1 tidal instability" by Lubow (1991). In addition to the superhumps, negative superhumps are often observed in various phases (from quiescent to superoutburst phases) of the disk evolution of dwarf novae. Recently, for example, Osaki and Kato (2013a) showed that the frequency of the negative superhump varies systematically during a supercycle (a cycle from one superoutburst to the next). The negative superhumps have been supposed to be due to disk tilt, but the origin of the tilt seems not to be understood yet, although many possibilities have been suggested, e.g., tidal instability (Lubow 1992), magnetic couplings between the disk and either the secondary or the primary (Murray et al. 2002), stream–disk interaction with a variable vertical stream component due

[7] The excitation of one-armed oscillation is considered to be the cause of superhumps in dwarf novae.

to asymmetric irradiation of the secondary (Smak 2009), and dynamical lift by the gas stream (Montgomery & Martin 2010). Our wave–wave resonant instability process is an extension of Lubow's tidal instability one (Lubow 1991, 1992). We think that further examination on this line is important for judging whether excitation of tilt by tidal instability can be regarded as one of the possible origins of negative superhumps.

Acknowledgments

The author thanks the referee for valuable suggestions, which greatly improved the paper.

Appendix 1. Trapping (capture) condition of tilt mode by the WKB method

We introduce the variable h_1, defined by $h_1 = p_1/\rho_0$, where p_1 is the pressure variation associated with oscillations over the unperturbed pressure $p_0(r, z)$, and $\rho_0(r, z)$ is the unperturbed density. Here, r and z are the r- and z-components of the cylindrical coordinates whose center is at the center of the primary star. The radial wavelength of oscillations is assumed to be moderately short. Then, we have a wave equation in terms of h_1 as (e.g., Kato 2001)

$$\frac{1}{\rho_0}\frac{\partial}{\partial z}\left(\rho_0\frac{\partial h_1}{\partial z}\right)+(\omega-m\Omega)^2\frac{\partial}{\partial r}\left[\frac{1}{(\omega-m\Omega)^2-\kappa^2}\frac{\partial h_1}{\partial r}\right]+\frac{(\omega-m\Omega)^2}{c_s^2}h_1=0, \tag{A1}$$

where $c_s(r)$ is the acoustic speed in the disk, and $m = 1$ in the present problem, since we are considering the tilt mode here.

Wave equations similar to equation (A1) have been solved by the WKB method, approximately separating $h_1(r, z)$ as $h_1(r, z) = g(\eta)f(r, \eta)$ (e.g., Silbergleit et al. 2001; Kato 2012). Here, η is defined by $\eta = z/H$ and $H(r)$ is the scale height of the disk half-thickness. After separating wave equation (A1) into two ordinary differential equations describing variations in the vertical and horizontal directions by use of g and f, we first solve the equation describing the variation in the vertical direction. The equation is the Hermite equation in the case of vertically isothermal disks. Boundary conditions at $z/H = \pm\infty$ gives us a discrete set of the separation constant, n, which is $n = 0, 1, 2, \ldots$ (e.g., Okazaki et al. 1997). Then, the equation describing the variations in the horizontal direction becomes

$$c_s^2\frac{d}{dr}\left[\frac{1}{(\omega-m\Omega)^2-\kappa^2}\frac{df}{dr}\right]+\frac{(\omega-m\Omega)^2-n\Omega_\perp}{(\omega-m\Omega)^2}f=0, \tag{A2}$$

where n is the separation constant mentioned above and $n = 1$ in the case of the tilt (and also $m = 1$).

By introducing $\tau(r)$ defined by

$$\tau(r)=\int_{r_i}^{r}\left\{[\omega-m\Omega(r')]^2-\kappa^2(r')\right\}dr', \tag{A3}$$

where r_i is the radius where an inner boundary condition is imposed, we can reduce equation (A2) to

$$\frac{d^2f}{d\tau^2}+Qf=0, \tag{A4}$$

where

$$Q(\tau)=\frac{(\omega-m\Omega)^2-n\Omega_\perp^2}{c_s^2(\omega-m\Omega)^2[(\omega-m\Omega)^2-\kappa^2]}. \tag{A5}$$

Equation (A4) is solved by the standard WBK method with the conditions that the outer trapping (capture) radius, r_{L1}, is a turning point of Q, and at the inner boundary the radial velocity vanishes. Then, the trapping condition is given by equation (11).

Appendix 2. Modes of tidal wave

The values of $n(\equiv \omega_D/\Omega_{orb})$ and m_D required for the tidal waves have been summarized in table 1. The subject to be considered here is whether such tidal waves really exist in tides and whether eccentricity of the orbit is required.

We consider the tidal perturbations induced at a position P($\boldsymbol{r}$) on the disk of the primary by a scondary star of mass M_s. When the point P is at a distance $R[= (r^2 + z^2)^{1/2}]$ from the center of the primary and the secondary star's zenith distance observed at the point P is ϑ (see figure 5), the tidal gravitational potential $\psi_D(\boldsymbol{r}, t)$ at the point P is

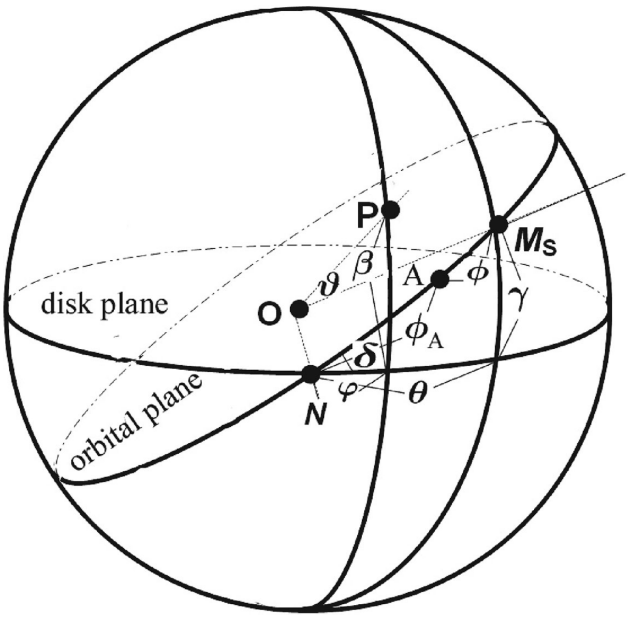

Fig. 5. Relation between disk plane and orbital plane of the secondary.

given by (e.g., Lamb 1924)

$$\psi_{\rm D} = -\frac{GM_{\rm s}}{(D^2 - 2RD\cos\vartheta + R^2)^{1/2}} + \frac{GM_{\rm s}}{D^2} R\cos\vartheta, \qquad \text{(A6)}$$

where D is the distance between the primary and secondary stars at time t. The second term on the right-hand side represents the potential of a uniform field of force of the secondary acting on the primary. Since D is larger than R, the right-hand side of equation (A6) is expanded by a power series of R/D as

$$\frac{\psi_{\rm D}}{GM_{\rm s}/D} = -1 - \left(\frac{R}{D}\right)^2 P_2(\cos\vartheta) - \left(\frac{R}{D}\right)^3 P_3(\cos\vartheta) - \cdots, \qquad \text{(A7)}$$

where $P_2(\cos\vartheta)$ and $P_3(\cos\vartheta)$ are the Legendre polynomials P_ℓ of argument $\cos\vartheta$ with $\ell = 2$ and $\ell = 3$, respectively. In the case where the orbit of the secondary is elliptical, D is a function of time. Hence, it is convenient to normalize $\psi_{\rm D}$ by a time-independent quantity. Here, we normalize $\psi_{\rm D}$ by the mean radius, a, of the elliptical orbit (see later for the relation between D and a) as

$$\frac{\psi_{\rm D}}{GM_{\rm s}/a} = -\frac{a}{D} - \left(\frac{R}{a}\right)^2 \left(\frac{a}{D}\right)^3 P_2(\cos\vartheta) - \left(\frac{R}{a}\right)^3 \left(\frac{a}{D}\right)^4 P_3(\cos\vartheta) - \cdots. \qquad \text{(A8)}$$

The next problem is to represent $P_2(\cos\vartheta)$ [and $P_3(\cos\vartheta)$] in terms of the cylindrical coordinates (r, φ, z) of the point P and coordinates (θ, γ) representing the position of the secondary on the revolutional orbit. As a preparation, we consider a unit sphere whose center is the center of the primary, as shown in figure 5. The poles of the sphere are taken in the direction perpendicular to the disk plane. The orbital plane of the secondary inclines to the disk plane by the angle δ. Let us denote the spherical coordinates of the point P by φ and β, as shown in figure 5. The angle φ is measured from the nodal point N. Then, using a formula of spherical trigonometry we have

$$\cos\vartheta = \sin\beta\sin\gamma + \cos\beta\cos\gamma\cos(\theta - \varphi). \qquad \text{(A9)}$$

Hence, simple algebraic calculations give

$$\begin{aligned} P_2(\cos\vartheta) &= \frac{1}{2}(3\cos^2\vartheta - 1) \\ &= \frac{1}{4}(3\sin^2\beta - 1)(3\sin^2\gamma - 1) \\ &\quad + \frac{3}{4}\sin 2\beta \sin 2\gamma \cos(\theta - \varphi) \\ &\quad + \frac{3}{4}\cos^2\beta\cos^2\gamma\cos[2(\theta - \varphi)], \end{aligned} \qquad \text{(A10)}$$

and

$$\begin{aligned} P_3(\cos\vartheta) &= \frac{1}{2}(5\cos^3\vartheta - 3\cos\vartheta) \\ &= \frac{1}{4}\sin\beta\sin\gamma \\ &\quad \times \left[25\sin^2\beta\sin^2\gamma - 15(\sin^2\beta + \sin^2\gamma) + 9\right] \\ &\quad + \frac{1}{8}\cos\beta\cos\gamma\left[75\sin^2\beta\sin^2\gamma + 3\right. \\ &\qquad \left. -15(\sin^2\beta + \sin^2\gamma)\right]\cos(\theta - \varphi) \\ &\quad + \frac{15}{4}\sin\beta\sin\gamma\cos^2\beta\cos^2\gamma\cos[2(\theta - \varphi)] \\ &\quad + \frac{5}{8}\cos^3\beta\cos^3\gamma\cos[3(\theta - \varphi)], \end{aligned} \qquad \text{(A11)}$$

where $P_2(\cos\vartheta)$ and $P_3(\cos\vartheta)$ have been expressed in terms of β, γ, and $\theta - \varphi$.

Here, θ and γ are related to δ and $\phi_{\rm A} + \phi$ by spherical trigonometric formulae:

$$\begin{aligned} \cos\gamma &= \cos(\phi_{\rm A} + \phi)\cos\theta + \sin(\phi_{\rm A} + \phi)\sin\theta\cos\delta, \\ \sin\gamma &= \sin(\phi_{\rm A} + \phi)\sin\delta, \end{aligned} \qquad \text{(A12)}$$

where $\phi_{\rm A}$ is the angular direction of periastron, A, measured from the nodal point N along the orbit of the secondary, and ϕ is the position of the secondary on the orbit, measured from the periastron, A (see figure 5). These relations (A12) show that in the limit of $\delta = 0$, we have $\gamma = 0$ and $(\phi_{\rm A} + \phi) = \theta$, as expected. Even when $\delta \neq 0$, the above relations (A12) show that $\sin\gamma = \delta\sin(\phi_{\rm A} + \phi)$ and $\phi_{\rm A} + \phi = \theta$ until the order of δ^2. Hence, in this paper, assuming that the misalignment between the disk and orbital planes is not large, we adopt

$$\theta = (\phi_{\rm A} + \phi), \quad \sin\gamma = \delta\sin(\phi_{\rm A} + \phi), \qquad \text{(A13)}$$

and the terms of the order of δ^2 are neglected in equations (A10) and (A11). Then, $P_2(\cos\vartheta)$ and $P_3(\cos\vartheta)$ are approximated at

$$\begin{aligned} P_2(\cos\vartheta) &\sim \frac{1}{4}(1 - 3\sin^2\beta) \\ &\quad + \frac{3}{4}\delta\sin 2\beta\left[\sin(2\phi + 2\phi_{\rm A} - \varphi) + \sin\varphi\right] \\ &\quad + \frac{3}{4}\cos^2\beta\cos\left[2(\phi + \phi_{\rm A} - \varphi)\right], \end{aligned} \qquad \text{(A14)}$$

Table 2. Time and azimuthal dependences of tidal waves in coplanar systems.

Separation	e^0	e^1	e^2
$(R/a)^2$	$2\Omega_{\rm orb}t-2\varphi$	$\Omega_{\rm orb}t-2\varphi$	-2φ
		$3\Omega_{\rm orb}t-2\varphi$	$2\Omega_{\rm orb}t-2\varphi$
			$4\Omega_{\rm orb}t-2\varphi$
$(R/a)^3$	$\Omega_{\rm orb}t-\varphi$	$-\varphi$	$-\Omega_{\rm orb}t-\varphi$
		$2\Omega_{\rm orb}t-\varphi$	$\Omega_{\rm orb}t-\varphi$
			$3\Omega_{\rm orb}t-\varphi$
	$3\Omega_{\rm orb}t-3\varphi$	$2\Omega_{\rm orb}t-3\varphi$	$\Omega_{\rm orb}t-3\varphi$
		$4\Omega_{\rm orb}t-3\varphi$	$3\Omega_{\rm orb}t-3\varphi$
			$5\Omega_{\rm orb}t-3\varphi$
$(R/a)^4$	$2\Omega_{\rm orb}t-2\varphi$	$\Omega_{\rm orb}t-2\varphi$	-2φ
		$3\Omega_{\rm orb}t-2\varphi$	$2\Omega_{\rm orb}t-2\varphi$
			$4\Omega_{\rm orb}t-2\varphi$
	$4\Omega_{\rm orb}t-4\varphi$	$3\Omega_{\rm orb}t-4\varphi$	$2\Omega_{\rm orb}t-4\varphi$
		$5\Omega_{\rm orb}t-4\varphi$	$4\Omega_{\rm orb}t-4\varphi$
			$6\Omega_{\rm orb}t-4\varphi$

Table 3. Time and azimuthal dependences of tidal waves added in coplanar systems with $\delta \ll 1$.

Separation	e^0	e^1	e^2
$(R/a)^2$	$-\varphi$	$-\Omega_{\rm orb}t-\varphi$	$-2\Omega_{\rm orb}t-\varphi$
		$\Omega_{\rm orb}t-\varphi$	$-\varphi$
			$2\Omega_{\rm orb}t-\varphi$
	$2\Omega_{\rm orb}t-\varphi$	$\Omega_{\rm orb}t-\varphi$	$-\varphi$
		$3\Omega_{\rm orb}t-\varphi$	$2\Omega_{\rm orb}t-\varphi$
			$4\Omega_{\rm orb}t-\varphi$
$(R/a)^3$	$\Omega_{\rm orb}t-2\varphi$	-2φ	$-\Omega_{\rm orb}t-2\varphi$
		$2\Omega_{\rm orb}t-2\varphi$	$\Omega_{\rm orb}t-2\varphi$
			$3\Omega_{\rm orb}t-2\varphi$
	$3\Omega_{\rm orb}t-2\varphi$	$2\Omega_{\rm orb}t-2\varphi$	$\Omega_{\rm orb}t-2\varphi$
		$4\Omega_{\rm orb}t-2\varphi$	$3\Omega_{\rm orb}t-2\varphi$
			$5\Omega_{\rm orb}t-2\varphi$
$(R/a)^4$	$2\Omega_{\rm orb}t-\varphi$	$\Omega_{\rm orb}t-\varphi$	$-\varphi$
		$3\Omega_{\rm orb}t-\varphi$	$2\Omega_{\rm orb}t-\varphi$
			$4\Omega_{\rm orb}t-2\varphi$
	$2\Omega_{\rm orb}t-3\varphi$	$\Omega_{\rm orb}t-3\varphi$	-3φ
		$3\Omega_{\rm orb}t-3\varphi$	$2\Omega_{\rm orb}t-3\varphi$
			$4\Omega_{\rm orb}t-3\varphi$
	$4\Omega_{\rm orb}t-3\varphi$	$3\Omega_{\rm orb}t-3\varphi$	$2\Omega_{\rm orb}t-3\varphi$
		$5\Omega_{\rm orb}t-3\varphi$	$4\Omega_{\rm orb}t-3\varphi$
			$6\Omega_{\rm orb}t-3\varphi$

and

$$P_3(\cos\vartheta) \sim -\frac{3}{4}\delta\sin\ \beta\ (5\sin^2\beta-3)\sin(\phi+\phi_{\rm A}) + \frac{1}{8}(3-15\sin^2\beta)\cos\beta\cos(\phi+\phi_{\rm A}-\varphi) + \frac{15}{8}\delta\sin\beta\cos^2\beta\,[\sin(3\phi+3\phi_{\rm A}-2\varphi) - \sin(\phi+\phi_{\rm A}-2\varphi)] + \frac{5}{8}\cos^3\beta\cos\,[3(\phi+\phi_{\rm A}-\varphi)]\,. \quad \text{(A15)}$$

In the limiting case where the secondary star's orbit is circular (i.e., $e=0$), ϕ is obviously $\phi=\Omega_{\rm orb}t$. Hence, in this case, if the orbital plane coincides with the disk plane (i.e., $\delta=0$), the tidal waves are two-armed ($m_{\rm D}=2$) with frequency $2\Omega_{\rm orb}$ (i.e., $\omega_{\rm D}=2\Omega_{\rm orb}$) [see equation (A14) and table 2], if the expansion in equation (A7) is terminated by the second term on the right-hand side. If the expansion proceeds to the next term, the one-armed ($m_{\rm D}=1$) tidal waves with frequency $\Omega_{\rm orb}$ and the three-armed ($m_{\rm D}=3$) tidal waves with frequency $3\Omega_{\rm orb}$ appear [see equation (A15) and table 2], but the ratio of $\omega_{\rm orb}/m_{\rm D}$ is still $\Omega_{\rm orb}$. In misaligned cases ($\delta\neq0$), the situations are changed and even when $e=0$, we have one-armed ($m_{\rm D}=1$) tidal waves with $\omega_{\rm orb}=2\Omega_{\rm orb}$ [see equation (A14) and table 3], and two-armed ($m_{\rm D}=2$) waves with $\omega_{\rm D}=\Omega_{\rm orb}$ and $\omega_{\rm D}=3\Omega_{\rm orb}$ [see equation (A15) and table 3]. That is, in these cases, the ratio $\omega_{\rm D}/m_{\rm D}$ is not always $\Omega_{\rm orb}$, but the ratio of $2\Omega_{\rm orb}$ and $(3/2)\Omega_{\rm orb}$ appears even if $e=0$.

Some tidal waves required to lead to resonant instability (see table 1), however, are still different from those tidal waves mentioned above. That is, the results in section 5 show that for some resonant instability to occur, other relations of $\omega_{\rm D}/m_{\rm D}$ are required. For such tidal waves to occur, the orbit of the secondary is needed to be eccentric. To examine this in detail, we must know i) the deviation of $\phi(t)$ from $\phi=\Omega_{\rm orb}t$ and ii) the time variation of a/D in the cases of elliptical orbits.

The functional form of $\phi(t)$ is well known in the fields of celestial mechanics. The main results concerning $\phi(t)$ are summarized as follows. Let the eccentricity and the mean radius of the orbit be e and a, respectively. Then, the distance of the secondary from the center of the primary, D, changes with a change of $\phi(t)$ as

$$D=\frac{a(1-e^2)}{1+e\cos\phi}. \quad \text{(A16)}$$

Now, we introduce an angle u (eccentric anomaly) defined by

$$D=a(1-e\cos u). \quad \text{(A17)}$$

Then, the equation of motion shows that the time variation of $u(t)$ is described by the Kepler equation:

$$u-e\sin u=\Omega_{\rm orb}t, \quad \text{(A18)}$$

where $u=0$ (and thus $\phi=0$) is taken at $t=0$. In the limit of the circular orbit ($e=0$), we have $D=a$ and $u=\phi=\Omega_{\rm orb}t$.

Equation (A18) is solved with respect to u by a power series of e, assuming that e is small. Then, we have (e.g., Araki 1980)

$$u = \Omega_{\rm orb}t + e\sin(\Omega_{\rm orb}t) + \frac{1}{2}e^2\sin(2\Omega_{\rm orb}t) + \frac{1}{8}e^3\left[3\sin(3\Omega_{\rm orb}t) - \sin(\Omega_{\rm orb}t)\right] + \cdots. \quad \text{(A19)}$$

Combining equations (A16) and (A17) gives $(1 + e\cos\phi)(1 + e\cos u) = (1 - e^2)$. From this equation and $\phi = \Omega_{\rm orb}t$ in the limit of $e = 0$, we obtain (e.g., Araki 1980)

$$\phi = \Omega_{\rm orb}t + 2e\sin(\Omega_{\rm orb}t) + \frac{5}{4}e^2\sin(2\Omega_{\rm orb}t) + \frac{1}{12}e^3\left[13\sin(3\Omega_{\rm orb}t) - 3\sin(\Omega_{\rm orb}t)\right] + \cdots. \quad \text{(A20)}$$

Furthermore, $a/D = (1 - e\cos u)^{-1}$ is also expanded by a power series of e as

$$\frac{a}{D} = 1 + e\cos u + e^2\cos^2 u + e^3\cos^3 u + \cdots. \quad \text{(A21)}$$

Then, by using equation (A19) we can write a/D explicitly as a function of $\Omega_{\rm orb}t$:

$$\frac{a}{D} = 1 + e\cos(\Omega_{\rm orb}t) + e^2\cos(2\Omega_{\rm orb}t) + \frac{1}{8}e^3\left[9\cos(3\Omega_{\rm orb}t) - \cos(\Omega_{\rm orb}t)\right]. \quad \text{(A22)}$$

If expressions for P_ℓ [equations (A14) and (A15)], a/D [equation (A22)], and ϕ [equation (A20)] are substituted into equation $\psi_{\rm D}$ [equation (A8)], we have $\psi_{\rm D}$ expressed directly in terms of the coordinates of the observing point, (φ, β), the secondary's orbital parameters ($\Omega_{\rm orb}$, e, a) and the inclination, δ, between the disk and orbital planes. The tidal waves generally have forms of $\cos[n\Omega_{\rm orb} - m_{\rm D}\varphi]$ or $\sin[n\Omega_{\rm orb} - m_{\rm D}\varphi]$. The phase $(n\Omega_{\rm orb} - m_{\rm D}\varphi)$ in various cases is shown in tables 2 and 3, by taking $m_{\rm D} > 0$.

References

Araki, T. 1980, MÉCANIQUE CÉLESTE (Tokyo: Kooseisha), 85 (in Japanese)
Ferreira, B., & Ogilvie, G. I. 2008, MNRAS, 386, 2297
Kato, S. 2001, PASJ, 53, 1
Kato, S. 2004, PASJ, 56, 905
Kato, S. 2008, PASJ, 60, 111
Kato, S. 2012, PASJ, 64, 78
Kato, S. 2013a, PASJ, 65, 56
Kato, S. 2013b, PASJ, 65, 75
Kato, S. 2014, PASJ, 66, 25
Kato, S., Fukue, J., & Mineshige, S. 2008, Black-Hole Accretion Disks—Towards a New Paradigm (Kyoto: Kyoto University Press), chap. 11
Kato, S., Okazaki, A. T., & Oktariani, F. 2011, 63, 363
Lamb, H. 1924, Hydrodynamics (Cambridge: Cambridge University Press), 336
Lubow, S. H. 1991, ApJ, 381, 259
Lubow, S. H. 1992, ApJ, 401, 317
Meyer-Vernet, N., & Sicardy, B. 1987, Icarus, 69, 157
Montgomery, M. M., & Martin, E. L. 2010, ApJ, 722, 989
Moritani, Y., et al. 2013, PASJ, 65, 83
Morse, P. M., & Feshbach, H. 1953, Methods of Theoretical Physics (New York: McGraw-Hill), chapter 9
Murray, J. R., Chakrabarty, D., Wynn, G. A., & Kramer, L. 2002, MNRAS, 335, 247
Okazaki, A. T., Kato, S., & Fukue, J. 1987, PASJ, 39, 457
Oktarian, F., Okazaki, A. T., & Kato, S. 2010, PASJ, 62, 709
Ohshima, T., et al. 2012, PASJ, 64, L3
Osaki, Y. 1985, A&A, 144, 369
Osaki, Y., & Kato, T. 2013a, PASJ, 65, 50
Osaki, Y., & Kato, T. 2013b, PASJ, 65, 95
Patterson, J., Jablonski, F., Koen, C., O'Donoghue, D., & Skillman, D. R. 1995, PASP, 107, 1183
Silbergleit, A. S., Wagoner, R. V., & Ortega-Rodrígues, M. 2001, ApJ, 548, 385
Smak, J. 2009, Acta Astron., 59, 419